Inorganic Chemistry Communications 12 (2009) 558–562

Contents lists available at ScienceDirect

Inorganic Chemistry Communications

journal homepage: www.elsevier.com/locate/inoche

Syntheses, topological analyses and magnetic properties of two 3D supramolecular nickel-organic frameworks constructed from 1,3,5-benzenetricarboxylate and flexible imidazole-based ligands

Jian-Di Lin [a,b], Cui-Cui Jia [a,b], Zhi-Hua Li [a], Shao-Wu Du [a,*]

[a] State Key Laboratory of Structural Chemistry, Fujian Institute of Research on the Structure of Matter, Chinese Academy of Sciences, Fuzhou, Fujian 350002, PR China
[b] Graduate University of Chinese Academy of Sciences, Beijing 100039, PR China

ARTICLE INFO

Article history:
Received 17 February 2009
Accepted 16 April 2009
Available online 24 April 2009

Keywords:
Metal-organic frameworks
Crystal structures
Topological analyses
Magnetic properties

ABSTRACT

Two supramolecular nickel-organic frameworks, $[Ni(HBTC)(bix)]_n$ (**1**) and $[Ni_3(BTC)_2(mbix)_3(H_2O)_4]_n \cdot 6nH_2O$ (**2**) (bix = 1,4-bis(imidazole-l-yl-methyl)benzene, *m*bix = 1,3-bis(imidazole-l-yl-methyl)benzene, and H_3BTC = 1,3,5-benzenetricarboxylate), have been hydrothermally prepared by the assembly of H_3BTC, Ni^{2+} with bix or *m*bix. Compound **1** shows a 2D layer structure, whose 3D supramolecular structure exhibits a **fsc** topology when hydrogen-bonging interactions between the adjacent layers are taken into account. Compound **2** manifests an unprecedented 2D (3, 4)-connected topological net. The 3D supramolecular framework of **2** is formed through $\pi\cdots\pi$ stacking interactions between the adjacent layers. The magnetic studies show that **1** features overall ferromagnetic property whilst **2** presents strong zero-field splitting (ZFS) when treated as a mononuclear model. Furthermore, the IR and TGA properties of **1** and **2** were also studied.

The design and synthesis of functional metal-organic frameworks (MOFs) have been received extensive attention in recent years owing to their potential as functional materials [1–4] and intriguing topologies [5–7]. Consequently, a variety of coordination polymers with complicated architectures and topologies have been synthesized successfully [8–10]. It is widely acknowledged that the coordinative bonding is normally considered to be the primary interaction to sustain the network, while those supramolecular interactions, such as hydrogen-bonding, $\pi\cdots\pi$ stacking interactions and metal–metal interactions are also expected to control the assembly and dimensionality of the resulting structures and direct the overall supramolecular topology [11–17]. The topological analysis could be a better insight into the supramolecular architectures. Upon topological analysis, complicated metal-organic frameworks can be reduced to simple equivalent networks [5].

According to our investigation, MOFs with 3-, 4-, or 6-connected topologies in which *d*-block metal ions are used as nodes are commonly observed [18]. However, the 3D frameworks with mixed connectivity, such as (3, 6)-, (4, 6)-, and (4, 8)-connected frameworks, are considered to be difficult to achieve because of their greater geometric limitations [18]. Our interests are focused on designing metal-organic frameworks using transition metal ions to assembly with mixed-ligands of polycarboxylates and flexible *N*-donor ligands and carrying out their topological analyses. In our knowledge, MOFs constructed from aromatic carboxylates and bix (bix = 1,4-bis(imidazole-l-yl-methyl)benzene) or *m*bix (*m*bix = 1,3-bis(imidazole-l-yl-methyl)benzene) have not been well explored [19–26]. Recently, we have successfully obtained five novel d^{10} metal-organic coordination polymers containing mixed ligands of polycarboxylates and bix (or *m*bix). These polymers exhibit different topologies from one to another, in which the polycarboxylate acids display their characteristic distinct coordination modes [27]. As part of our ongoing effort in the design of topological architecture, we have investigated the assemblies of Ni ion and the mixed-ligands of H_3BTC (H_3BTC = 1,3,5-benzenetricarboxylate) and bix (or *m*bix), which led to the isolation of two 3D supramolecular MOFs, $[Ni(HBTC)(bix)]_n$ (**1**) and $[Ni_3(BTC)_2(mbix)_3(H_2O)_4]_n \cdot 6nH_2O$ (**2**). The crystal structures, topological analyses, thermal stability of these compounds, along with their magnetic properties will be represented and discussed in this paper.

Bix and *m*bix were synthesized by the literature method [28]. All the other chemicals were commercially available and used as purchased. $NiCl_2 \cdot 6H_2O$ (0.125 mmol, 29.7 mg), H_3BTC (0.125 mmol, 26.3 mg), bix (0.25 mmol, 59.5 mg), and H_2O (10 mL) were placed in a Teflon-lined stainless steel vessel and the mixture was sealed and heated to 130 °C for 72 h. The reaction system was cooled to room temperature during 36 h. Green prism crystals of **1** were obtained, yield: 39 mg, 62% based on $NiCl_2 \cdot 6H_2O$. Blue prism crystals of **2** were obtained in a similar way as for **1** except that *m*bix was employed instead of bix and the reaction

* Corresponding author. Tel./fax: +86 591 83709470.
E-mail address: swdu@ms.fjirsm.ac.cn (S.-W. Du).

1387-7003/$ - see front matter © 2009 Elsevier B.V. All rights reserved.
doi:10.1016/j.inoche.2009.04.020

temperature was 160 °C, yield: 29.8 mg, 48% based on $NiCl_2 \cdot 6H_2O$. *Elemental analysis* (%) Anal. Calc. For compound **1** ($C_{23}H_{18}NiN_4O_6$): Calcd. C 54.69, H 3.59, N 11.09; Found: C 54.67, H 3.18, N 11.15(%) and for compound **2** ($C_{60}H_{68}Ni_3N_{12}O_{22}$): Calcd. C 48.52, H 4.61, N 11.32; Found: C 48.91, H 4.58, N 11.36(%). Empirical absorption corrections were applied to the data using the CrystalClear program [29]. The structures of **1** and **2** were solved by the direct method and refined by the full-matrix least-squares on F^2 using the SHELXTL-97 program [30]. All of the non-hydrogen atoms were refined anisotropically. The hydrogen atoms of organic ligands in **1** and **2** were treated by geometrical positions or located from difference Fourier maps. The hydrogen atoms of lattice and coordinated water molecules in **2** were not added. Crystallographic data and structural refinements for compounds **1** and **2** are summarized in Table S1. The selected bond distances and bond angles for compound **1** and **2** are summarized in Table S2 and Table S3, respectively. The IR spectra of **1** (Figure S1) and **2** (Figure S2) show the characteristic bands of the carboxylic groups in the usual region at 1457–1343 cm^{-1} for the symmetric vibrations and at 1630–1535 cm^{-1} for the asymmetric vibrations. The presence of the characteristic band attributed to the protonated carboxylic group is observed at 1720 cm^{-1} for **1**, indicating the incomplete deprotonation of the H_3BTC ligand.

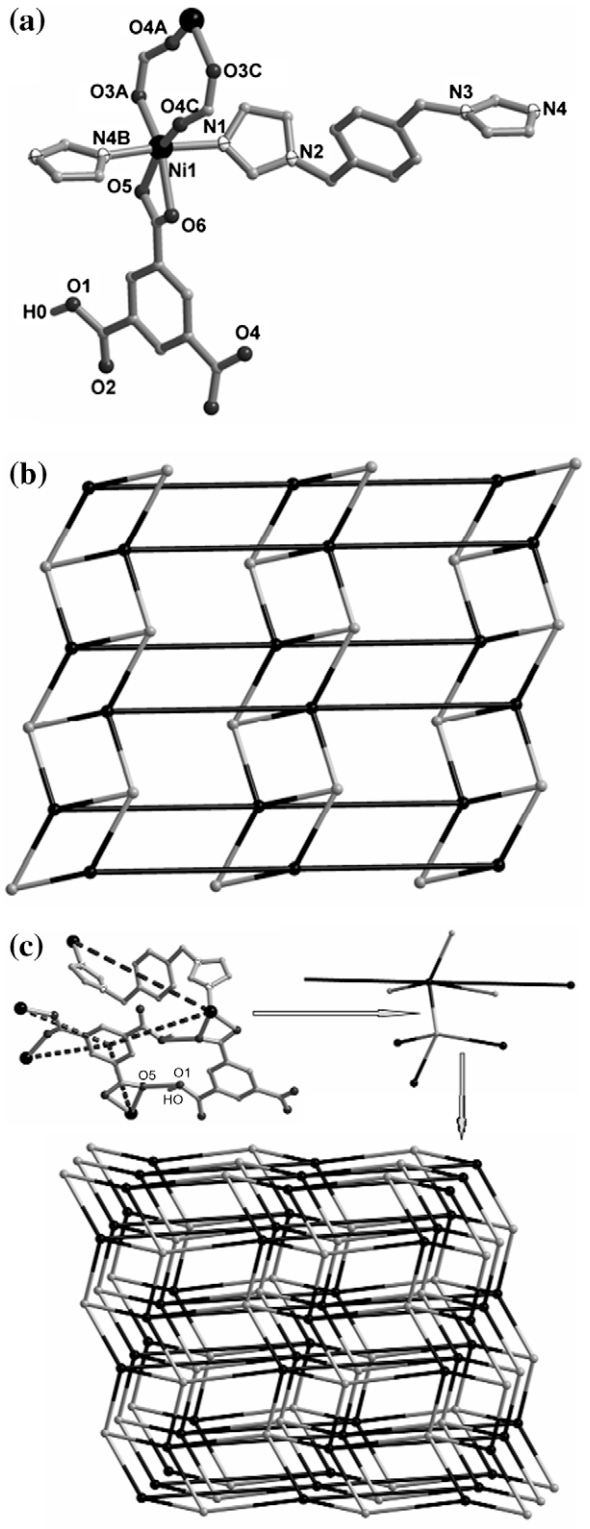

Fig. 1. (a) View of the coordination environment of Ni ion in **1**. Symmetry codes: (A) $x, y+1, z$; (B) $x-1, y, z-1$; (C) $-x, -y, -z+2$. Hydrogen atoms belonged to C atoms are omitted for clarity. (b) View of the 2D topological network in **1**. (c) View of the 3D topological network in **1**.

Compound **1** crystallizes in the triclinic space group *P*–1 and the asymmetric unit contains one Ni ion, one bix and one $HBTC^{2-}$ anion. There exists one carboxyl group in the $HBTC^{2-}$ anion. As shown in Fig. 1a, the Ni1 centre is in a distorted octahedral coordination geometry, and is coordinated by two nitrogen atoms from two distinct bix ligands (N1, N4B), two carboxylate oxygen atoms in a bidentate mode from two symmetry-related $HBTC^{2-}$ ligands (O3A, O4C) and one chelating carboxylate oxygen atoms (O5, O6) from another $HBTC^{2-}$ ligand. The Ni–O/N bond lengths are all in the normal range [31]. The bond angles around Ni1 centre range from 60.71(4) to 169.65(6)°. The two nitrogen atoms occupy the axial positions of the octahedron with the N1–Ni1–N4B bond angle of 169.65(6)°, whereas the equatorial plane of the distorted octahedral sphere is defined by the four carboxylate oxygen atoms. The Ni1 center is approximately coplanar with the mean plane of the four equatorial oxygen atoms with a deviation of 0.0191 Å Chart 1.

The $HBTC^{2-}$ ligand employs one chelating carboxylate group and one bidentate carboxylate group, adopting a (k^2)-$(k^1$-$k^1)$-μ_3 coordination mode (Chart 2a), to connect the Ni ions into a 1D double chain motif with alternating 8-membered (A) and 16-membered (B) rings (Figure S3), which are common arrangements found in other transition metal carboxylate complexes [23,32–35]. The

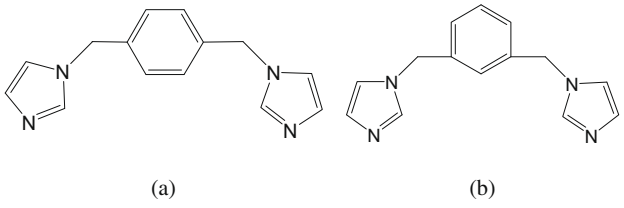

Chart 1.

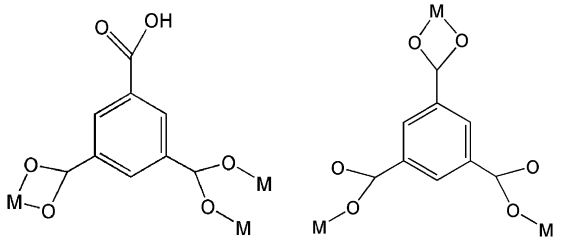

Chart 2.

distance of the two Ni atoms in A ring is 4.4950(5) Å. The flexible bix ligands bridge the metal centres of the 1D double chains in an *anti*-conformation to build up a 2D layer (Figure S4). The dihedral angle between two terminal imidazole rings is 43.79°. Finally, these 2D layers are further extended into a 3D supramolecular architecture with channels through strong hydrogen bonds involving the uncoordinated carboxylate group and the chelating carboxylate group [O1–H0···O5#1 2.706 Å; symmetry code: (#1) –*x*, –*y*, 1 – *z*], as illustrated in Figure S5.

From the topological point of view, the 2D layer in **1** is a (3, 5)-connected net. The long connection is corresponding to a bix bridge. Each Ni1 atom acts as a five-connected node and every $HBTC^{2-}$ ligand functions as a 3-connected node in the ratio 1:1 (Fig. 1b). The 2D net is analyzed by OLEX program [36] and the result shows that the Schläfli symbol can be described as $(4^2 \cdot 6)(4^2 \cdot 6^7 \cdot 8)$. The vertex symbol of the 3-connected node and the five-connected node in this 2D net is $4 \cdot 4 \cdot 6_2$ and $4 \cdot 4 \cdot 6_4 \cdot 6_4 \cdot 6_3 \cdot 6_3 \cdot 6_3 \cdot 6_3 \cdot {}^{*} \cdot {}^{*}$, respectively. To the best of our knowledge, there is only one example of 2D topological net with Schläfli symbol of $(4^2 \cdot 6)(4^2 \cdot 6^7 \cdot 8)$ reported to date [37]. If the hydrogen-bonding interactions are taken into account [38,39], the $HBTC^{2-}$ ligand can be regarded as a 4-connected node. Therefore, the connectivity of **1** can be simplified as a (4, 6)-connected 3D network and the overall Schläfli symbol becomes $(4^4 \cdot 6^2)(4^4 \cdot 6^{10} \cdot 8)$ (Fig. 1c). The 4-connected node and 6-connected node of this 3D net can be further specified by the vertex symbol of

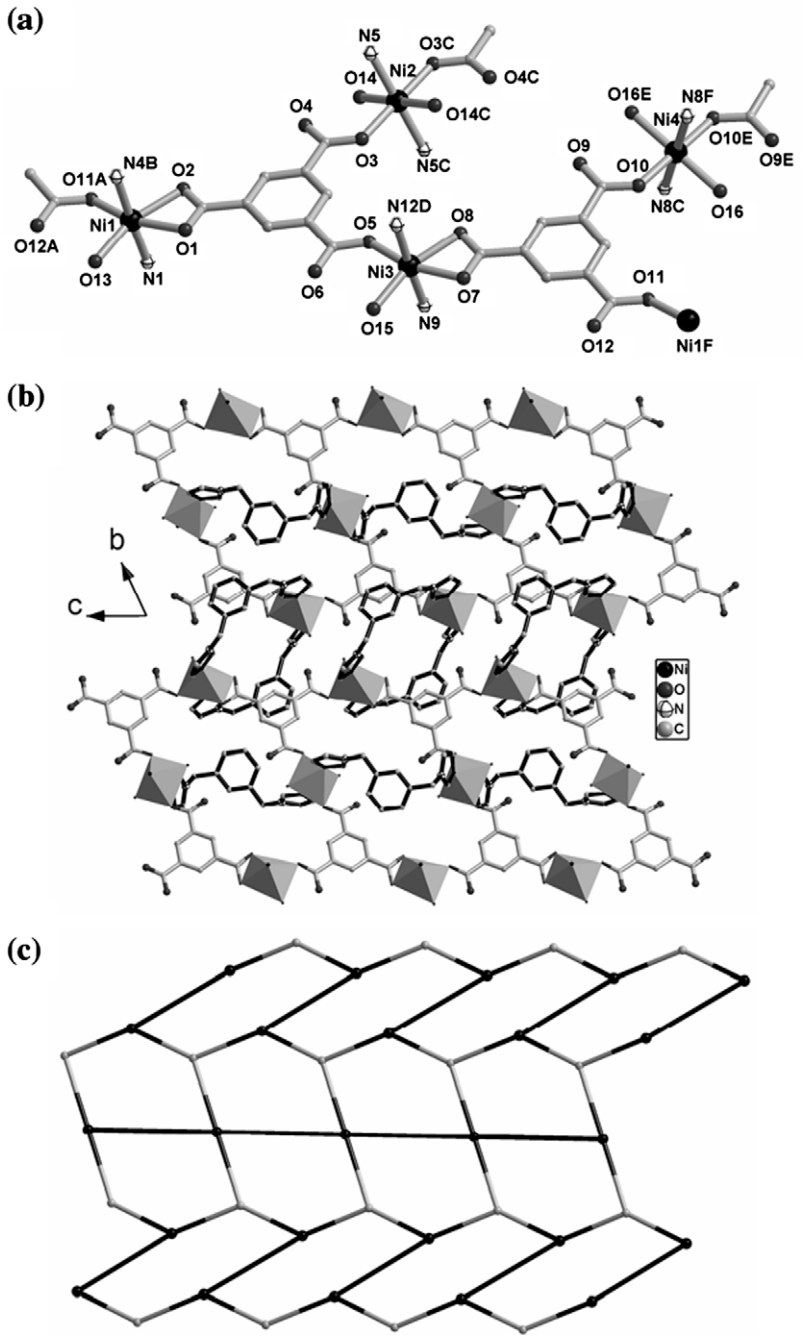

Fig. 2. (a) View of the coordination environment of Ni ions in **2**. (b) Polyhedral view of the 2D layer structure in **2**. The zigzag chain and 24-membered rings are highlighted in black. Lattice water molecules are omitted for clarity. (c) View of the 2D topological network in **2**. Hydrogen atoms are omitted for clarity. Symmetry codes: (A) *x*, *y*, *z* − 1; (B) −*x* − 1, −*y*, −*z* + 1; (C) −*x* − 2, −*y* + 1, −*z* + 1; (D) −*x* − 1, −*y*, −*z* + 2; (E) −*x* − 2, −*y* + 1, −*z* + 2; (F) *x*, *y*, *z* + 1.

$4\cdot4\cdot4\cdot4\cdot6_2\cdot6_2$ and $4\cdot4\cdot4\cdot4\cdot6_5\cdot6_5\cdot6_5\cdot6_5\cdot6_5\cdot6_5\cdot6_5\cdot6_5\cdot{}^{*}{}^{*}{}^{*}$, respectively. According to O'Keeffe, this net with Schläfli symbol $(4^4\cdot6^2)(4^4\cdot6^{10}\cdot8)$ is named as **fsc** net [36]. The coordination sequences of this fsc net are 4, 16, 38, 66, 102, 146, 198, 258, 326, 402 for the 4-connected node and 4, 18, 38, 66, 102, 146, 198, 258, 326, 402 for the 6-connected node [40]. As far as we know, metal-organic frameworks with the **fsc** topology have been rarely encountered [41].

The asymmetric unit of **2** contains four crystallographically independent Ni atoms, two kinds of unique BTC^{3-} ligands, three kinds of unique *m*bix ligands, and four coordinated water molecules and six lattice water molecules. All the Ni atoms are six-coordinated. The Ni1 (or Ni3) is coordinated by three carboxylate oxygen atoms from two BTC^{3-}, two nitrogen atoms from two *m*bix ligands and a water molecule. In the distorted octahedral sphere of Ni1 and Ni3 centres, the four oxygen atoms make up of the equatorial plane, whereas the two nitrogen atoms locate at the axial positions of the octahedron. The bond angles of N1–Ni1–N4B and N9–Ni3–N12D are 178.22(9) and 176.84(9)°, respectively (Fig. 2a). The Ni1 and Ni3 centres are approximately coplanar with the mean plane of their four equatorial oxygen atoms with a deviation of 0.0572 and 0.0359 Å, respectively. As for Ni2 and Ni4 centres, they are both surrounded by one monodentate carboxylate oxygen atom from BTC^{3-}, one nitrogen atom from *m*bix and one water molecule along with their corresponding symmetry-related atoms (Fig. 2a). The arrangement sequences of the coordination atoms around Ni2 and Ni4 are similar to that of Ni1 and Ni3. All the coordination bonds are in normal distances [31].

Each BTC^{3-} ligand utilizes one chelating carboxylate group and two monodentate carboxylate groups, adopting a (k^2)-(k^1)-(k^1)-μ_3 coordination mode (Chart 2b), to join the Ni ions into a 1D ladder structure (Figure S6). Three crystallographically distinct *m*bix ligands in **2** all adopt a *syn*-conformation with the dihedral angles between two terminal imidazole rings varying from 19.465° to 81.161°. The Ni2 and Ni4 along with their corresponding symmetry-related atoms are linked by a *m*bix ligand to form an infinite zigzag chain with the distance of Ni2···Ni4 being 10.1750(2) Å. The other two *m*bix ligands each form a 24-membered ring via coordination to Ni1 or Ni3 with the distances of Ni1···Ni1B and Ni3···Ni3D being 8.2014(6) and 7.9828(5) Å, respectively (Figure S7). The zigzag chains pass through the centres of the 1D ladders, which are further extended by the 24-membered rings to produce a 2D layer structure (Fig. 2b). Close $\pi\cdots\pi$ contacts occur between aromatic rings of BTC^{3-} and the phenyl rings of *m*bix ligands of the adjacent layers with face-to-face distance of 3.6519 Å (with centroid-to-centroid distance of 3.935 Å). Thus, the structure of **2** can also be described as a 3D supramolecular network (Figure S8). If the *m*bix ligands are considered as connectors, and both crystallographically independent BTC^{3-} ligands are simplified as 3-connected nodes, there exist two kinds of 3-connected nodes (Ni1/Ni3 and BTC^{3-}) and one kind of 4-connected node (Ni2/Ni4). The topology of this 2D network can be described as a (3, 4)-connected net (Fig. 2c). Therefore, the Schläfli symbol of this net is $(5\cdot6^2)(5^2\cdot6)(5^4\cdot8^2)$. To the best of our knowledge, the 2D metal-organic frameworks with this topology net are previously unknown.

In comparison, when different symmetries of flexible imidazole-based ligands (bix and *m*bix) were employed as coligands to construct **1** and **2**, absolutely distinct frameworks and topologies are emerged in these metal-organic frameworks. In **1**, twofold deprotonated $HBTC^{2-}$ ligand employs two carboxylate groups, adopting a (k^2)-$(k^1$-$k^1)$-μ_3 coordination mode (Chart 2a). Whereas in **2**, the coordination mode of triply deprotonated BTC^{3-} ligand is (k^2)-(k^1)-(k^1)-μ_3 (Chart 2b), utilizing all the three carboxylate groups.

The thermal stability of **1** and **2** was examined by TGA in a nitrogen atmosphere. The TGA curve of **1** (Figure S9) indicates that there is no significant loss up to about 370 °C. The TGA curve of **2** (Figure S10) reveals a weight loss of 7.31% from room temperature to 134 °C, which can be assigned to the weight loss of the lattice water molecules (calcd = 7.27%). The subsequent weight loss of 4.76% from 134 °C to 343 °C can be attributed to the weight loss of the coordinated water molecules (calcd = 4.85%). And from 343 °C the decomposition of the framework of **2** starts.

The temperature-dependent magnetic susceptibility data of **1** and **2** have been measured for polycrystalline samples at an applied magnetic field of 10 kOe in the temperature range of 2–300 K, as shown in Fig. 3. For **1**, χ_m is the molar magnetic susceptibility for per Ni_2 unit (A ring in Figure S3). The experimental χ_mT value at room temperature is 2.45 $cm^3\ mol^{-1}$ K, which is as expected for two magnetically quasi-isolated $S = 1$ ions ($g > 2.00$). Upon cooling, the χ_mT value increases to a maximum of 3.12 $cm^3\ mol^{-1}$ K at 5.55 K, following with a sharp decrease to 2.56 $cm^3\ mol^{-1}$ K at 2 K, suggesting an overall ferromagnetic interaction. Fitting all data to the Curie–Weiss law gave Weiss constant of $\theta = 3.42$ K (Figure S11), also indicative of ferromagnetic exchange interactions. With the consideration of the intermolecular exchange interaction (ZJ') in the molecular-field approximation, the magnetic analysis was carried out by using the spin Hamiltonian $H = -2JS_1S_2 - D(S_1^2 + S_2^2)$, where J is the intramolecular exchange integral, D the zero-field splitting parameter. And the expression of magnetic susceptibility reported in the literature can be used to fit the data [42]. A good fit was achieved with the fitting parameters as follows: $g = 2.204$, $J = +2.70\ cm^{-1}$, $D = -0.035\ cm^{-1}$, $ZJ' = -0.133\ cm^{-1}$ and the agreement factor $R = \Sigma[(\chi_mT)_{obsd} - (\chi_mT)_{calcd}]^2/\Sigma(\chi_mT)^2_{obsd}$ is 1.28×10^{-4}.

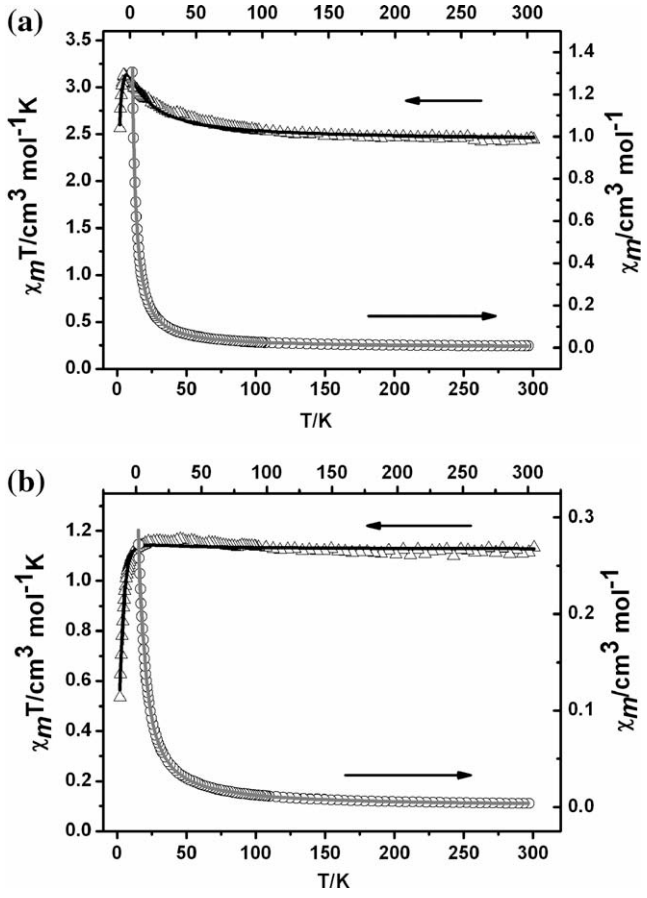

Fig. 3. Temperature dependence of χ_mT (▽)and χ_m (○) values for **1** (a) and **2** (b). The solid lines correspond to the best-fit curves using the parameters described in the text.

For **2**, the experimental $\chi_m T$ value for per Ni ion at room temperature is 1.11 $cm^3\ mol^{-1}\ K$ and increase slowly to a maximum of 1.16 $cm^3\ mol^{-1}\ K$ at 22.5 K. Below 22.5 K, there is a clear decrease to approximately 0.53 $cm^3\ mol^{-1}\ K$ at 2 K. Although the structure of **2** is two-dimensional, from the magnetic point of view, it can be analyzed with a mononuclear model owing to the long Ni···Ni distances between the organic linkers. The resulting magnetic susceptibility is given by Eq. (1), where θ represents all the weak interactions and the other symbols have their usual meanings. The best fitting gave the parameters $g = 2.12$, $D = 12.67$ K, $\theta = 0.747\ K^{-1}$ and the agreement factor $R = \Sigma[(\chi_m T)_{obsd} - (\chi_m T)_{calcd}]^2/\Sigma(\chi_m T)^2_{obsd}$ is 1.3×10^{-4}. The decrease of $\chi_m T$ value below 22.5 K might be mainly attributed to the presence of zero-field splitting (ZFS).

$$\chi_m = \frac{2Ng^2\beta^2}{3k(T-\theta)}\left[\frac{2kT/D - 2kT\exp(-D/kT)/D + \exp(-D/kT)}{1 + 2\exp(-D/kT)}\right] \quad (1)$$

In summary, we have successfully obtained two nickel-organic frameworks using mixed-ligand of H_3BTC and bix (or *m*bix) under hydrothermal conditions. Compounds **1** and **2** both exhibit a 3D supramolecular network with a novel topology formed by hydrogen-bonging interactions or $\pi\cdots\pi$ stacking interactions. The different symmetries of bix and *m*bix play an important role in tuning the formation of the network structures of **1** and **2**. The magnetic study shows that **1** exhibits an overall ferromagnetic interaction between the Ni^{2+} ions whereas **2** presents strong zero-field splitting (ZFS) based on the magnetic analysis result.

Acknowledgements

This work was supported by the Grants from the State Key Laboratory of Structural Chemistry, Fujian Institute of Research on the Structure of Matter, Chinese Academy of Sciences (CAS, SZD08002-2), National Basic Research Program of China (973 Program, 2007CB815306), the National Natural Science Foundation of China (20733003 and 20673117) and Knowledge Innovation Program of the Chinese Academy of Sciences.

Appendix A. Supplementary material

Supplementary data associated with this article can be found, in the online version, at doi:10.1016/j.inoche.2009.04.020.

References

[1] G.J. Halder, C.J. Kepert, B. Moubaraki, K.S. Murray, J.D. Cashion, Science 298 (2002) 1762.
[2] C.N.R. Rao, S. Natarajan, R. Vaidhyanathan, Angew. Chem., Int. Ed. 43 (2004) 1466.
[3] O.M. Yaghi, H. Li, C. Davis, D. Richardson, T.L. Groy, Acc. Chem. Res. 31 (1998) 474.
[4] S.R. Batten, B.F. Hoskins, B. Moubaraki, S. Murray, K.R. Robson, Chem. Commun. (2000) 1095.
[5] N.W. Ockwig, O. Delgado-Fridrichs, M. O'Keeffe, O.M. Yaghi, Acc. Chem. Res. 38 (2005) 176.
[6] V.A. Blatov, L. Calucci, D.M. Proserpio, J. Am. Chem. Soc. 127 (2005) 1504.
[7] D. Bradshaw, J.B. Claridge, E.J. Cussen, T.J. Prior, M.J. Rosseinsky, Acc. Chem. Res. 38 (2005) 273.
[8] S.R. Batten, CrystEngComm 3 (2001) 67.
[9] O.M. Yaghi, M. O'Keeffe, N.W. Ockwig, H.K. Chae, M. Eddaoudi, J. Kim, Nature 423 (2003) 705.
[10] R.J. Hill, D.-L. Long, N.R. Champness, P. Hubberstey, M. Schröder, Acc. Chem. Res. 38 (2005) 337.
[11] A.J. Blake, N.R. Champness, P. Hubberstey, W.S. Li, M.A. Withersby, M. Schröder, Coord. Chem. Rev. 183 (1999) 117.
[12] D.B. Leznoff, B.Y. Xue, R.J. Batchelor, F.W.B. Einstein, B. Patrick, Inorg. Chem. 40 (2001) 6026.
[13] M. Munakata, L.P. Wu, T. Kuroda-Sowa, Adv. Inorg. Chem. 46 (1999) 173.
[14] A.M. Beatty, Coord. Chem. Rev. 246 (2003) 131.
[15] O.M. Yaghi, H. Li, T.L. Groy, Inorg. Chem. 36 (1997) 4292.
[16] M. Fujita, Y.J. Kwon, S. Washizu, K. Ogura, J. Am. Chem. Soc. 116 (1994) 1151.
[17] C.L. Chen, C.Y. Su, Y.P. Cai, H.X. Zhang, A.W. Xu, B.S. Kang, H.C. Zur Loye, Inorg. Chem. 42 (2003) 3738.
[18] M. Du, Z.H. Zhang, L.F. Tang, X.G. Wang, X.J. Zhao, S.R. Batten, Chem. Eur. J. 13 (2007) 2578.
[19] L.L. Wen, Y.Z. Li, Z.D. Lu, J.G. Lin, C.Y. Duan, Q.J. Meng, Cryst. Growth Des. 6 (2006) 530.
[20] L.L. Wen, D.B. Dong, C.Y. Duan, Y.Z. Li, Z.F. Tian, Q.J. Meng, Inorg. Chem. 44 (2005) 7161.
[21] L.L. Wen, Z.D. Lu, J.G. Lin, Z.F. Tian, H.Z. Zhu, Q.J. Meng, Cryst. Growth Des. 7 (2007) 93.
[22] Z.D. Lu, L.L. Wen, Z.P. Ni, Y.Z. Li, H.Z. Zhu, Q.J. Meng, Cryst. Growth Des. 7 (2007) 268.
[23] Y.Y. Liu, J.F. Ma, J. Yang, Z.M. Su, Inorg. Chem. 46 (2007) 3027.
[24] Z.F. Tian, J.G. Lin, Y. Su, L.L. Wen, Y.M. Liu, H.Z. Zhu, Q.J. Meng, Cryst. Growth Des. 7 (2007) 1863.
[25] X.Y. Duan, Y.Z. Li, Y. Su, S.Q. Zang, C.J. Zhu, Q.J. Meng, CrystEngComm 9 (2007) 758.
[26] Y. Qi, F. Luo, Y.X. Che, J.M. Zheng, Cryst. Growth Des. 8 (2008) 606.
[27] J.D. Lin, J.W. Cheng, S.W. Du, Cryst. Growth Des. 8 (2008) 3345.
[28] B.F. Hoskins, R. Robson, D.A. Slizys, J. Am. Chem. Soc. 119 (1997) 2952.
[29] Molecular Structure Corporation & Rigaku, 2000. CrystalClear, Version 1.36. MSC, 9009 New Trails Drive, The Woodlands, TX 77381-5209, USA, and Rigaku Corporation, 3-9-12 Akishima, Tokyo, Japan.
[30] SHELXTL (version 5.10), Siemens Analytical X-ray Instruments Inc., Madison, WI, 1994.
[31] E.Y. Choi, Y.U. Kwon, Inorg. Chem. 44 (2005) 538.
[32] X.J. Li, R. Cao, W.H. Bi, Y.Q. Wang, Y.L. Wang, X. Li, Z.G. Guo, Cryst. Growth Des. 5 (2005) 1651.
[33] C. Ma, C. Chen, Q. Liu, D. Liao, L. Li, L. Sun, New J. Chem. 27 (2003) 890.
[34] L.M. Duan, F.T. Xie, X.Y. Chen, Y. Che, Y.K. Lu, P. Cheng, J.Q. Xu, Cryst. Growth Des. 6 (2006) 1101.
[35] X.L. Hong, Y.Z. Li, H.M. Hu, Y. Pan, J.F. Bai, X.Z. You, Cryst. Growth Des. 6 (2006) 1221.
[36] O.V. Dolomanov, A.J. Blake, N.R. Champness, M. Schröder, J. Appl. Crystallogr. 36 (2003) 1283.
[37] Y.Q. Sun, J. Zhang, G.Y. Yang, Chem. Commun. (2006) 1947.
[38] D.R. Xiao, R. Yuan, Y.Q. Chai, E.B. Wang, Eur. J. Inorg. Chem. (2008) 2610.
[39] J.J. Jiang, Y.R. Liu, R. Yang, M. Pan, R. Cao, C.Y. Su, CrystEngComm 10 (2008) 1147.
[40] See website: http://rcsr.anu.edu.au/.
[41] M.H. Bi, G.H. Li, J. Hua, Y.L. Liu, X.M. Liu, Y.W. Hu, Z. Shi, S.H. Feng, Cryst. Growth Des. 7 (2007) 2066.
[42] Q.L. Wang, L.H. Yua, D.Z. Liao, S.P. Yan, Z.H. Jiang, P. Cheng, Helv Chim Acta 86 (2003) 2441.